III Cu atoms are in fact arranged in a novel trinuclear cluster, liganded by a total of eight His side chains. There are three β-barrel domains, each with folding characteristic of the cupredoxins. One domain supplies four of the His ligands to the novel trinuclear center, one is devoid of Cu, and the third both binds the type I Cu and supplies four histidines to the trinuclear cluster as well. The β-barrel core of domain I of NIR can be superimposed on domain III of AO. Moreover, with the same rotation and translation, domain II of the neighboring molecule superimposes on domain I of AO. The type I Cu and its ligands in NIR fall at the type I site of AO, and all three of the histidines of the type II site, as well as the Cu, fall in the same site as the trinuclear cluster of AO (Fig. 5). Sequence comparison (*13*) shows that two His from domain I (residues 100 and 135) and two from domain II (residues 255 and 306) correspond to four of the eight ligand His in AO. In NIR only His residues 100, 135, and 306 are ligands. These comparisons suggest that Cu-II of NIR corresponds to one of the type III Cu pair in AO. At an atomic level, the interaction between molecules in NIR resembles the interaction between domains in AO.

The location of catalytic metal at an interface of two otherwise not covalently linked polypeptide chains is rare. One case is the Fe center in the photoreaction center of *Rhodopseudomonas viridis* (*23*). In that case two His ligands come from the L chain and two His and a carboxylate come from the M chain. This Fe center lies deep in that assembly and is not likely to be involved in any interaction with substrate.

Hulse and colleagues have shown that the production of NO or N_2O from this enzyme proceeds through a nitrosyl (E-NO^+) intermediate (*24*). The absence of a fourth protein ligand for the type II Cu suggests that the intermediate would form at this Cu. Suzuki *et al.* (*25*) have reported that the EPR signal of both the *Alcaligènes sp.* (NCIB 11015) NIR (with only type I Cu) and the *Achromobacter* NIR is reversibly lost upon binding NO, suggesting that only the type I site is involved. However, in view of the similarity of the location of the type II Cu to the active site in AO, we believe it is unlikely that the type I Cu in NIR is sufficient for activity. Denariaz *et al.* (*3*) have documented one of the highest specific activities for *A. cycloclastes* NIR.

We have crystallized NIR in the presence of an excess of NO_2^- resulting in a brownish-pink crystal that is isomorphous with the native crystal. Difference density maps showed changes at each Cu site interpretable as NO_2^- displacing the water ligand at Cu-II and a partial loss of Cu at the Cu-I site. A more extensive exploration of these differences as well as a higher pH crystal form of native protein should help further elucidate the mechanism of NIR.

REFERENCES AND NOTES

1. W. Payne, in *Dentrification in the Nitrogen Cycle*, H. L. Golterman, Ed. (Plenum, New York, 1985), pp. 47–65.
2. H. L. Golterman, *ibid.*, pp. 1–6.
3. G. Denariaz, W. J. Payne, J. LeGall, *Biochim. Biophys. Acta* **1056**, 255 (1991).
4. M.-Y. Liu, M.-C. Liu, W. Payne, J. LeGall, *J. Bacteriol.* **166**, 604 (1986).
5. H. Iwasaki, S. Noji, S. Shidara, *J. Biochem.* **78**, 355 (1975).
6. D. M. Dooley, R. S. Moog, M.-Y. Liu, W. J. Payne, J. LeGall, *J. Biol. Chem.* **263**, 14625 (1988).
7. H. Iwasaki and T. Matsubara, *J. Biochem.* **71**, 645 (1972).
8. J. P. Shapleigh and W. J. Payne, *FEMS Microbiol. Lett.* **26**, 275 (1985).
9. J. P. Shapleigh, K. J. P. Davies, W. J. Payne, *Biochim. Biophys. Acta* **911**, 334 (1987).
10. T. Kakutani, H. Watanabe, K. Arima, T. Beppu, *J. Biochem.* **89**, 463 (1981).
11. M. A. Kashem, H. B. Dunford, M.-Y. Liu, W. J. Payne, J. LeGall, *Biochem. Biophys. Res. Commun.* **145**, 563 (1989).
12. S. Turley *et al.*, *J. Mol. Biol.* **200**, 417 (1988).
13. F. F. Fenderson *et al.*, *Biochemistry* **30**, 7180 (1991).
14. The monomer of NIR crystallizes (*12*) in a cubic unit cell, $P2_13$, $a = b = c = 98.4$ Å. Data to 2.0 Å for a native crystal (in a stabilizing mother liquor consisting of 0.1 M sodium acetate at pH 5.2 and 36% saturated ammonium sulfate), and a $K_2Pt(SCN)_6$ derivative were collected at the UCSD area detector facility. A 2.0 Å data set for a uranyl $[UO_2(NO_3)_2]$ derivative was collected on a Siemens area detector in our laboratory. Anomalous scattering data were incomplete for the Pt derivative, so that solvent-flattening methods [B. C. Wang, *Methods Enzymol.* **115**, 90 (1985)] were used to resolve the phase ambiguity. The heavy-atom sites of the uranyl derivative were located from a difference Fourier calculated with these protein phases (Table 1). The uranyl derivative appeared to become non-isomorphous at higher resolution, so phasing was not carried out beyond 2.3 Å.
15. T. A. Jones, *Methods Enzymol.* **115**, 157 (1985).
16. A. T. Brünger, G. M. Clore, A. M. Gronenborn, M. Karplus, *Proc. Natl. Acad. Sci. U.S.A.* **83**, 3801 (1986).
17. C. I. Brändén and T. A. Jones, *Nature* **343**, 687 (1990).
18. E. T. Adman, in *Metalloproteins Part 1: Metal Proteins with Redox Roles*, P. M. Harrison, Ed. (Macmillan, London, 1985), pp. 1–42.
19. M. L. Connolly, *J. Appl. Crystallogr.* **16**, 548 (1983).
20. E. I. Solomon, in *Copper Coordination Chemistry*, K. D. Karlin, and J. Zubieta, Eds. (Adenine, New York, 1983), pp. 1–22.
21. M. W. Parker, F. Pattus, A. D. Tucker, D. Tsernoglou, *Nature* **337**, 93 (1989).
22. A. Messerschmidt *et al.*, *J. Mol. Biol.* **206**, 513 (1989).
23. J. Diesenhofer and H. Michel, *Science* **245**, 1463 (1989).
24. C. L. Hulse, J. M. Tiedje, B. A. Averill, *Anal. Biochem.* **172**, 420 (1988).
25. S. Suzuki *et al.*, *Biochem. Biophys. Res. Commun.* **164**, 1366 (1989).
26. D. C. Teller, *Methods Enzymol.* **27D**, 346 (1973).

27. Supported by NIH grants no. GM31770 and no. GM08268-02. The use of the area detector facility at UCSD is gratefully acknowledged. We thank A. Messerschmidt (Max Planck Institute, Munich) for release of α carbon and copper-ligand coordinates of ascorbate oxidase prior to deposition. The unrefined α carbon, copper, and ligand coordinates of the MIR model of NIR have been deposited with the Protein Data Bank (entry number 1NRD).

5 April 1991; accepted 4 June 1991

Recognition of a Cell-Surface Oligosaccharide of Pathogenic *Salmonella* by an Antibody Fab Fragment

MIROSLAW CYGLER,* DAVID R. ROSE, DAVID R. BUNDLE

The 2.05 angstrom (Å) resolution crystal structure of a dodecasaccharide-Fab complex revealed an unusual carbohydrate recognition site, defined by aromatic amino acids and a structured water molecule, rather than the carboxylic acid and amide side chains that are features of transport and other carbohydrate binding proteins. A trisaccharide epitope of a branched bacterial lipopolysaccharide fills this hydrophobic pocket (8 Å deep by 7 Å wide) in an entropy-assisted association (association constant = 2.05 × 10^5 liters per mole, enthalpy = −20.5 ± 1.7 kilojoules per mole, and temperature times entropy = +10.0 ± 2.9 kilojoules per mole). The requirement for the complementarity of van der Waals surfaces and the requirements of saccharide-saccharide and protein-saccharide hydrogen-bonding networks determine the antigen conformation adopted in the bound state

OLIGOSACCHARIDE EPITOPES OF bacterial and tumor cell-surface carbohydrates are important disease markers (*1*) and targets for therapeutic antibodies (*2*), but to date a crystal structure for an antibody-carbohydrate complex has not yet been reported. Consequently, appreciation of this molecule recognition has been limited to binding site models inferred from functional group replacement in conjunction with immunochemical mapping studies (*3*) and modeling of published binding sites (*4*).

We report the 2.05 Å resolution crystal structure of a carbohydrate epitope bound to a Fab fragment from a mouse monoclonal antibody. The antigen chosen for this study

M. Cygler, Biotechnology Research Institute, National Research Council of Canada, Montréal, Québec H4P 2R2, Canada.
D. R. Rose and D. R. Bundle, Institute of Biological Sciences, National Research Council of Canada, Ottawa, Ontario K1A 0R6, Canada.

*To whom correspondence should be addressed.

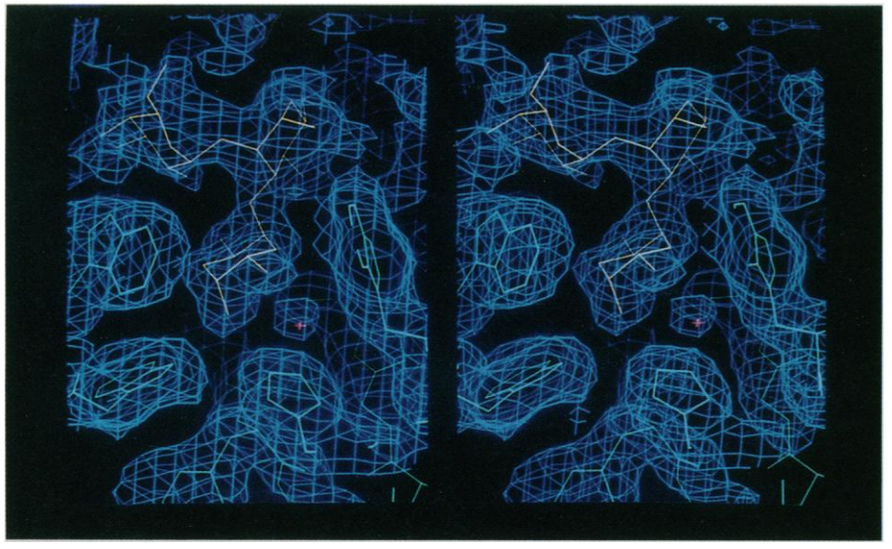

Fig. 1. The simulated annealing omit map in the region of antigen. The oligosaccharide and all residues within 6.0 Å were removed from the model, and the remaining atoms were refined by slow cooling protocol (*12*) from 800 to 300 K. The atoms in a 4.0 Å buffer zone near the removed atoms have been additionally restrained to their starting positions by harmonic potential.

was the polysaccharide O-antigen that is anchored to the outer membrane of pathogenic *Salmonella* of serogroup B. This organism is responsible for ~50% of gastrointestinal *Salmonella* infections in Europe and North America. Its O-antigen is built from repeating units containing four sugars, D-mannose (D-Man), D-galactose (D-Gal), L-rhamnose (L-Rha), and a 3,6-dideoxy-D-galactose (abequose, D-Abe) that forms a single branch unit (*5*).

$$\{\rightarrow 3)\alpha\text{D-Gal}(1 \rightarrow 2)[\alpha\text{D-Abe}(1 \rightarrow 3)]$$
$$\alpha\text{D-Man}(1\rightarrow 4)\alpha\text{L-Rha}(1\rightarrow\}_n$$

Although the abequose was prominent in early immunochemical studies (*6*), most carbohydrate epitopes do not contain this sugar (*1*).

The immune response to *Salmonellae* lipopolysaccharide antigen is dominated by epitopes involving 3,6-dideoxy derivatives of D-galactose (serogroup B), D-glucose (paratose, serogroup A), and D-mannose (tyvelose, serogroup D), structural features (*6*) that correlate with serological classification of *Salmonellae* (*7*). The conformational properties of the monomeric and oligomeric forms of these antigens in aqueous solution have been investigated by potential energy calculations and nuclear magnetic resonance measurements (*8, 9*).

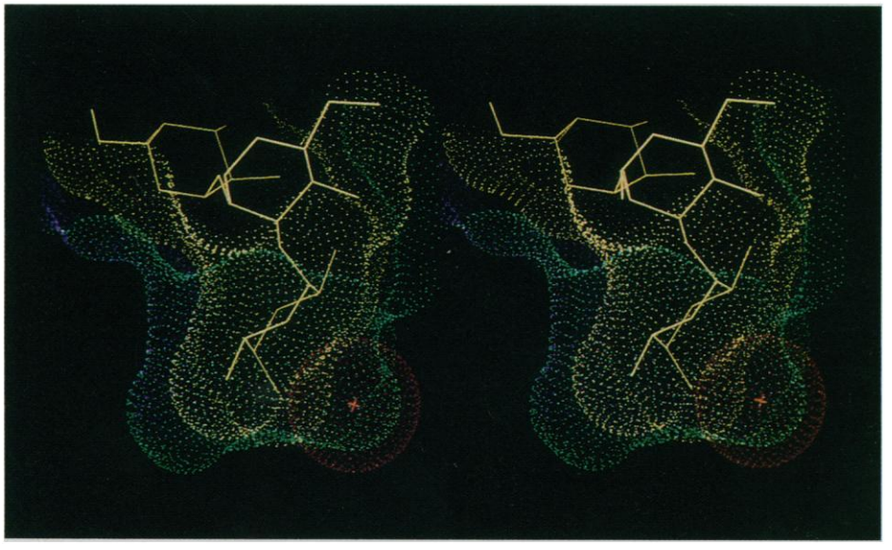

Fig. 2. Contact surfaces of the Fab and oligosaccharide, buried on formation of the complex. The pocket in the V-domain is filled with antigen. Calculations were performed with the program MS (*15*). The surface of an internal water molecule is shown in red.

The antibody Se155-4 used in this study belongs to the immunoglobulin IgG1(λ) subclass. Se155-4 precipitated the polysaccharide antigen from serogroup B *Salmonella*, indicating that it bound epitopes distributed along the polysaccharide chain. Immunoassays using synthetic glycoconjugates prepared from tetrasaccharide hapten αD-Gal(1 → 2)[αD-Abe(1 → 3)]αD-Man(1 → 4)αL-Rha and the analogous trisaccharide lacking rhamnose located the exact portion of the polysaccharide that comprised the epitope and suggested that the rhamnose residue contributed little to the binding energy because the association constant for each was $2.0 \pm 0.35 \times 10^5$ liter/mol. This result was confirmed by the thermodynamics of binding determined by titration microcalorimetry (*10*). The methyl glycoside of the trisaccharide αD-Gal(1 → 2)[αD-Abe(1 → 3)]αD-Man and a series of phage-derived oligosaccharides (*10*) that contain from two to five repeating units show a nearly constant binding energy of 31 ± 2.1 kJ/mol. For the trisaccharide, ~10 ± 2.9 kJ/mol arose from favorable entropy changes ($T\Delta S$, where T is temperature and ΔS is change in entropy). Furthermore, substitution of either tyvelose or paratose for abequose gave inactive compounds, indicating that the stereochemistry of the dideoxyhexose was crucial for binding.

The complex of Fab with the dodecasaccharide (three repeating units of the serogroup B oligosaccharide) was crystallized at pH = 7.5 with the use of polyethylene glycol 8000 as a precipitate (*11*). The space group was $P2_12_12_1$, with cell dimensions of a = 47.3 Å, b = 128.6 Å, and c = 79.5 Å. Diffraction data were collected on the San Diego Multiwire Systems area detector to 2.05 Å resolution [98% complete, 82.6% reflections with intensities $I > 2\sigma(I)$]. The starting model for the molecular replacement was taken from the structure of Se155-4 complexed with one repeating unit of serogroup B oligosaccharide, which was solved at low resolution in our laboratory (*11*).

The refinement was carried out by the simulated annealing algorithm (*12*) with manual refitting after each refinement cycle (*13*). To avoid model bias, the complementarity determining regions (CDR) were removed from the model at an early stage and were gradually rebuilt during the course of the refinement by following the connectivity of the electron density map. At this stage, we examined the difference map to locate the oligosaccharide. Three sugar units, abequose, mannose, and galactose, were fitted

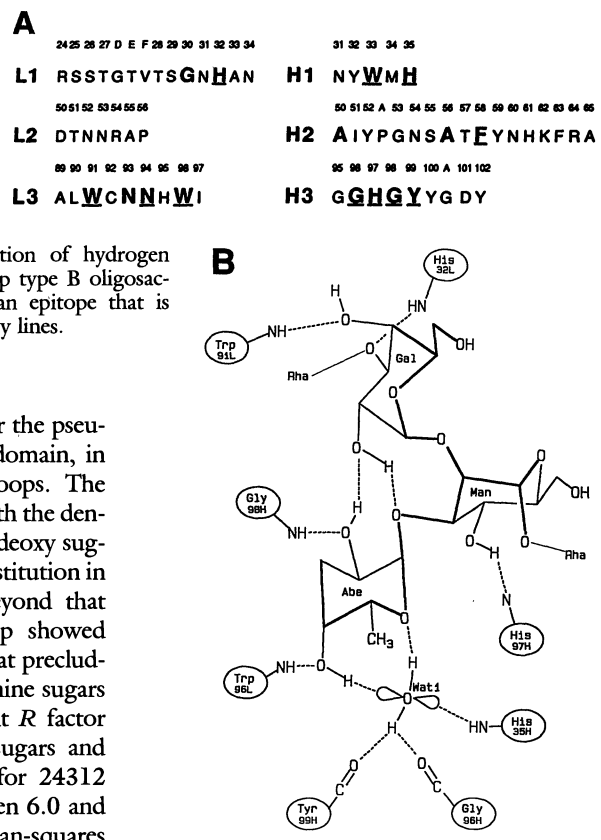

Fig. 3. (**A**) Sequences of CDR regions of Se155-4 antibody shown in one-letter code (*28*). Bold letters indicate residues contributing to the Fab surface buried by the antigen. Underlined letters show residues within 4.0 Å of the oligosaccharide. The amino acid sequences of the λ_1 and Fd chains were determined by protein sequencing method (*25*). (**B**) Schematic representation of hydrogen bonds involving *Salmonella* serogroup type B oligosaccharide. The αD-Gal[αD-Abe]αD-Man epitope that is visible in the crystal is shown in heavy lines.

into a large region of density near the pseudo twofold axis of the variable domain, in close proximity to the CDR loops. The assignment was unambiguous, with the density assigned for abequose, the dideoxy sugar, clearly showing the lack of substitution in positions 3 and 6 (Fig. 1). Beyond that region the electron density map showed scattered, unconnected density that precluded positioning of the remaining nine sugars with any confidence. The current *R* factor for the model including three sugars and ~80 water molecules is 0.185 for 24312 reflections with $I > 2\sigma(I)$ between 6.0 and 2.05 Å resolution. The root-mean-squares deviation for bond lengths is 0.014 Å and for bond angles is 2.9°.

The disposition of CDRs in the Fab creates a pocket approximately 8 Å deep and 7 Å wide. This site is occupied by abequose, the sugar that forms the branching residue of the polymer chain. It becomes totally buried, whereas mannose and galactose lie on the protein surface (Fig. 2) and are partially exposed to the solvent. The general direction of the oligosaccharide chain, as inferred from the placement of galactose and mannose, is roughly perpendicular to the variable light chain–variable heavy chain (V_L-V_H) interface. The shapes of the oligosaccharide and the antibody surfaces that are in contact with each other are highly complementary. The buried surface area [calculated with a 1.7 Å probe radius and van der Waals radii taken from (*14*) with the program MS (*15*)] on the Fab fragment is 304 Å^2, whereas that on the oligosaccharide is 255 Å^2. The largest contribution comes from abequose (121 Å^2) and the smallest from mannose (56 Å^2). The contact area is similar to that observed in a Fab fragment of an antibody to fluorescein (*16*), somewhat smaller than that observed in an antibody to peptide (*17*), and much smaller than the buried area in Fab-lysozyme complexes (750 Å^2) (*18*).

The Fab surface in contact with the antigen is defined by 15 CDR residues (Fig. 3A). Twelve of these are less than 4.2 Å from the oligosaccharide and make significant van der Waals interactions (Tables 1 and 2). Both hydrogen bonds and hydrophobic interactions are important for binding. The majority of contacts is provided by abequose. All sugar hydroxyl groups, with the exception of those at galactose C-6 and mannose C-6, participate in protein-carbohydrate hydrogen bonds (Fig. 3B). The most crucial hydrogen bonds are likely those that are buried deep in the binding pocket and involve O-2, O-4, and O-5 of abequose. Here the role of a buried water molecule (Wat 1) is pivotal. In addition to coordinating four hydrogen bonds (one bifurcated), it enhances Fab-antigen surface complementarity. Two hydrogen bonds with the protein anchor Wat 1, and Wat 1 accepts hydrogen bonds from O-4 of abequose and donates to the ring O-5 oxygen atom (Fig. 3B). The C-2 hydroxyl of abequose accepts a hydrogen bond from Gly 98H and, in turn, forms an intrasaccharide hydrogen bond to O-2 of galactose. In the light of these sterically demanding interactions, it is easily appreciated that this binding site fails to bind polysaccharide antigens that carry the D-manno- or D-gluco-3,6-dideoxyhexose isomers. In contrast to the arabinose binding protein (*19*), aromatic amino acid side chains dominate the Fab hydrogen bonding scheme.

The hydroxyl groups involved in hydrogen bonds are located toward one face of the epitope, and the hydrophobic environment for the nonpolar surfaces of the antigen is provided by stacking of Trp 91L against atoms C-3, C-4, C-5, and C-6 of abequose and C-1 and C-2 of galactose, and stacking of Trp 33H against C-6 of abequose and C-3 of mannose in a manner similar to that observed in the L-arabinose binding protein (*19*), lysozyme, and phosphorylase (*20*). This stacking also serves to sterically discriminate antigens that contain 3,6-dideoxy-D-glucose, the C-4 epimer of abequose.

Although the antigen binds near the local twofold axis of the V_L-V_H interface, 60% of all van der Waals contacts are with the VH domain. Four of the six CDRs, L1, L3, H1, and H3, make numerous contacts with the antigen, whereas H2, although it contributes to the formation of the binding pocket, interacts only weakly with the antigen (Fig. 3A). In contrast to large antigens such as lysozyme (*18*), the L2 makes no contacts with the antigen and makes no contribution to the binding. This seems to be a common feature of the binding of small haptens (*16, 17*).

The conformation observed for the bound trisaccharide epitope, αD-Gal(1 → 2)[αD-Abe(1 → 3)]αD-Man, lies within 14

Table 1. Van der Waals contacts between the oligosaccharide and Fab fragment (including ordered water). The numbers of atom-atom contacts <4.2 Å are shown in parentheses.

Sugar	Fab residues or ordered water
Gal	His 32L1 (7), Trp 91L3 (15), Asn 94L3 (2), His 97H3 (1)
Man	Trp 33H1 (3), His 97H3 (7), Ser 202H* (2)
Abe	Trp 91L3 (9), Trp 96L3 (6), Trp 33H1 (13), His 35H1 (4), Phe 58H2 (2), Gly 96H3 (4), His 97H3 (4), Gly 98H3 (5), Tyr 99H3 (1) Wat 1 (7)

*Contacts to residue from symmetry-related molecule.

Table 2. Hydrogen-bond contacts between the oligosaccharide and Fab fragment and ordered water.

Antigen atom	Contacting atom	Distance (Å)
Gal, O-2	O-1, Abe	3.00
Gal, O-2	O-2, Abe	2.68
Gal, O-3	Nε2, His 32L1	3.01
Gal, O-4	Nε1, Trp 91L3	3.04
Man, O-4	Nδ1, His 97H3	3.21
Abe, O-2	N, Gly 98H3	2.68
Abe, O-4	Nε1, Trp 96L3	2.86
Abe, O-4	O, Wat 1	2.84
Abe, O-5	O, Wat 1	3.11

kJ/mol of the calculated global minimum energy conformer (*8*). Whereas the glycosidic torsion angles of the αD-Abe(1 → 3)αD-Man linkage in the bound epitope agree reasonably well with the predicted values (ϕ, ψ of 80°, 91°, versus calculated values of 66°, 106°, where ϕ = O5-C1-O1-C′*x*, and ψ = C1-O1-C′*x*-C′*x*+1), the torsion angle of the αD-Gal(1 → 2)αD-Man linkage adopts a ϕ value that is shifted about 40° (ϕ, ψ of 105°, 83° versus calculated values of 68°, 101°) from the value of 60° to 70° that is generally anticipated from a consideration of the exo-anomeric effect (*21*) and is observed in crystal structures of methyl glycosides and oligosaccharides (*22*). The ϕ angle adopted by the galactose-mannose linkage is essential for an intramolecular scheme of conjugated hydrogen bonds that begin at Gly 98H and connect O-2 of abequose, O-2 of galactose, and O-1 of abequose. Potential energy calculations that include a hydrogen-bonding term indicate that unfavorable stereoelectronic and nonbonded interactions that result from the changed ϕ angle are offset by the intersaccharide hydrogen bonds.

In response to this bacterial antigen, the immune system has used somatic mutation of germ line genes (seven residues in the λ CDRs) to generate a carbohydrate binding site that is notably different from those previously investigated by crystallography. Although polar and planar side chains of the dicarboxylic amino acids have been identified as main features of hydrogen-bonding networks to sugars in carbohydrate binding proteins (*19*), this site is almost exclusively defined by aromatic amino acids. This result confirms inferences about the increased frequency of the use of aromatic amino acids in antibody CDRs (*23*). The abequose and the mannose are hydrogen-bonded to the side chains of His and Trp residues. The presence of three His residues in the CDRs contacting the saccharide probably results in the unusually mild dissociation pH, which corresponds to an approximate His pK_a of 5.6. At present, there is no way to differentiate between the three His residues that contact the epitope, but two of the imidazole rings (His 35H and His 97H) are thought to be neutral in the crystal.

This crystal structure shows that binding sites that use neutral amino acid hydrogen-bonding partners can have relatively high affinity for oligosaccharide epitopes. The conformation seen in the bound state, although fairly well modeled by simple potential energy calculations, is strongly influenced by the requirements for highly complementary surfaces and hydrogen-bonding networks (*19*). Hydroxyl groups that act as hydrogen-bond acceptors must also successfully donate a hydrogen bond to a neighboring acceptor (*24*). Here the functional groups that fulfill this role are a water molecule, other hydroxyl groups, and ring or exocyclic oxygen atoms occurring in acetal linkages. The inferred hydrogen-bonding scheme is also consistent with functional group replacement studies (*25*). The crystal structure described here, in combination with the use of synthetic gene technology to clone and express this Fab (*26*) and its fully active single-chain Fv fragment (*27*), provides the opportunity to engineer carbohydrate binding sites and to explore the importance of the different hydrogen-bond types for the stability of the carbohydrate-protein complexes.

REFERENCES AND NOTES

1. J. B. Robbins, *Immunochemistry* **15**, 839 (1978); J. Thurin, *Curr. Top. Microbiol. Immunol.* **139**, 59 (1988).
2. A. N. Houghton *et al.*, *Proc. Natl. Acad. Sci. U.S.A.* **82**, 1242 (1985).
3. C. P. J. Glaudemans, *Mol. Immunol.* **24**, 371 (1987); R. U. Lemieux, R. Cromer, U. Spohr, *Can. J. Chem.* **66**, 3083 (1988); R. U. Lemieux, *Chem. Soc. Rev.* **18**, 347 (1989).
4. E. M. Nashel *et al.*, *J. Biol. Chem.* **265**, 20699 (1990); E. A. Padlan and E. A. Kabat, *Proc. Natl. Acad. Sci. U.S.A.* **85**, 6885 (1988).
5. D. R. Bundle, *Top. Curr. Chem.* **154**, 1 (1990).
6. O. Lüderitz, A. M. Staub, O. Westphal, *Bacteriol. Rev.* **30**, 192 (1966).
7. F. Kauffmann, *The Bacteriology of Enterobacteriaceae* (Munksgaard, Copenhagen, 1966).
8. K. Bock *et al.*, *Carbohydr. Res.* **130**, 23 (1984).
9. K. Bock *et al.*, *ibid.*, p. 35.
10. B. Sigurskjold, E. Altman, D. R. Bundle, *Eur. J. Biochem.* **197**, 239 (1991).
11. D. R. Rose *et al.*, *J. Mol. Biol.* **215**, 489 (1990).
12. A. T. Brunger, X-plor, A System for Crystallography and NMR, 2.1, manual (Yale University, New Haven, CT, 1990).
13. A. T. Jones, *J. Appl. Crystallogr.* **11**, 614 (1978).
14. D. A. Case and M. Karplus, *J. Mol. Biol.* **132**, 343 (1979).
15. M. L. Connolly, *J. Appl. Crystallogr.* **16**, 548 (1983).
16. J. N. Herron, X.-M. He, M. L. Mason, E. W. Voss, Jr., A. B. Edmundson, *Proteins* **5**, 271 (1989).
17. R. L. Stanfield, T. M. Fieser, R. A. Lerner, I. A. Wilson, *Science* **248**, 712 (1990).
18. A. G. Amit, R. A. Mariuzza, S. E. V. Phillips, R. J. Poljak, *ibid.* **233**, 747 (1986); S. Sheriff *et al.*, *Proc. Natl. Acad. Sci. U.S.A.* **84**, 8075 (1987); E. A. Padlan *et al.*, *ibid.* **86**, 5938 (1989).
19. F. A. Quiocho, *Annu. Rev. Biochem.* **55**, 287 (1986).
20. L. N. Johnson *et al.*, *Curr. Top. Microbiol. Immunol.* **139**, 81 (1988).
21. R. U. Lemieux, S. Koto, D. Voisin, *ACS Symp. Ser.* **87**, 17 (1979).
22. S. Pérez and R. H. Marchessault, *Carbohydr. Res.* **65**, 114 (1978).
23. E. A. Padlan, *Proteins* **7**, 112 (1990).
24. F. A. Quiocho, D. K. Wilson, N. K. Vyas, *Nature* **300**, 404 (1989).
25. D. R. Bundle, unpublished results.
26. N. N. Anand *et al.*, *Gene*, in press.
27. N. N. Anand *et al.*, *J. Biol. Chem.*, in preparation.
28. Abbreviations for the amino acid residues are as follows: A, Ala; C, Cys; D, Asp; E, Glu; F, Phe; G, Gly; H, His; I, Ile; K, Lys; L, Leu; M, Met; N, Asn; P, Pro; Q, Gln; R, Arg; S, Ser; T, Thr; V, Val; W, Trp; and Y, Tyr.
29. National Research Council publication 32764.

4 February 1991; accepted 30 April 1991

Solution Structure of Kistrin, a Potent Platelet Aggregation Inhibitor and GP IIb-IIIa Antagonist

MARC ADLER, ROBERT A. LAZARUS, MARK S. DENNIS, GERHARD WAGNER*

The structure of kistrin, which is a member of a homologous family of glycoprotein IIb-IIIa (GP IIb-IIIa) antagonists and potent protein inhibitors of platelet aggregation, has been determined by two-dimensional nuclear magnetic resonance (NMR) spectroscopy. The 68-residue protein consists of a series of tightly packed loops held together by six disulfide bonds and has almost no regular secondary structure. Kistrin has an Arg-Gly-Asp (RGD) adhesion site recognition sequence important for binding to GP IIb-IIIa that is located at the apex of a long loop across the surface of the protein.

KISTRIN IS A POTENT PROTEIN INhibitor of platelet aggregation that occurs naturally and has recently been isolated from the venom of the Malayan pit viper *Agkistrodon rhodostoma* (*1*). Platelet aggregation is mediated by the interaction of a surface GP IIb-IIIa with plasma fibrinogen (Fg) and leads to the formation of platelet-rich clots, the inhibition of which may have beneficial affects for arterial thrombotic diseases (*2*). GP IIb-IIIa is a member of a family of glycoproteins called integrins, which are a large class of cell surface receptors that play important roles in cell-matrix and cell-cell adhesion (*3, 4*). Extracellular matrix ligands such as Fg, fibronectin, vitronectin, or von Willlebrand factor that bind to GP IIb-IIIa and other integrins all contain the RGD adhesion site recognition sequence thought to be critical

M. Adler and G. Wagner, Department of Biological Chemistry and Molecular Pharmacology, Harvard Medical School, Boston, MA 02115.
R. A. Lazarus and M. S. Dennis, Department of Protein Engineering, Genentech, Inc., South San Francisco, CA 94080.

*To whom correspondence should be addressed.